

eeMC: Arbitrary Initial Spin States for the Production of $e^+e^- \rightarrow \tau^+\tau^-(\gamma)$ Events and the Impact on Spin Correlations.

Ian M. Nugent*
Victoria, B.C., Canada

Abstract

We present a modified spin algorithm, including spin correlations, which has been implemented in eeMC for the simulation of $e^+e^- \rightarrow \tau^+\tau^-(\gamma)$ events with an arbitrary initial spin configuration. This algorithm is suitable for the proposed BELLE-II polarization upgrade to SuperKEKB [1, 2], both for the ideal case and for the case where there are misalignments, radiative effects and allows for changing polarization conditions. The spin 1/2 states of the polarized beams are constructed in terms of a super-positioning of the helicity states corresponding to the polarimetric-vector describing the overall beam polarization and implemented both through a modification of the initial state in the modified Altarelli-Parisi Density Function as well as a change of basis of the helicity states.

Keywords: Tau Lepton, Electron-Positron Collider, Monte-Carlo Simulation, Polarized Beams

1 Introduction

Recent proposals for an upgrade to SuperKEKB for polarization measurements at the BELLE-II experiment using a polarized e^- beam are motivated by precision electro-weak measurements of the $\sin^2\theta_W$ using the right-left asymmetry from pair production of e^+e^- , $\mu^+\mu^-$, $\tau^+\tau^-$, $c\bar{c}$ and $b\bar{b}$, measurements of the Michel Parameters, Tau electric-dipole-moment, Tau $g-2$ and the potential enhancements of new physics models [1, 2]. In the proposed upgrade to the SuperKEK design [1], the e^- beam circles the ring with a polarization vector along the vertical (y) axis, orthogonal to the KEK-ring plane, and is only rotated longitudinally along the e^- beam direction near the interaction point (IP). There are three proposed designs for rotating the spin axis: the BINP Spin Rotator Concept; Dipole-Solenoid-Quadrupoles combined function Magnets; and Direct Wind Magnets for the Spin Rotators [1]. Within these proposed design concepts, the longitudinal polarization is expected to reach $\sim 70 - 80\%$, however, the transverse components are not necessarily eliminated at the interaction point [1]. To evaluate the impact of the spin dynamic for polarized beams on experimental measurements, is it essential to be able incorporate the initial state spin dynamics for a broad range of accelerator and detector conditions, this includes mis-alignments, spin relaxation distributions and radiative effect, into the simulation for the determination of the efficiency and for evaluating the impact on physics observables in a given analysis. An algorithm which satisfies these criteria and which can be modified on an event-by-event biases is described in the following sections.

2 Overview of Generator Formalism

eeMC [3], is a stand-alone MC Generator which includes the random-number generation [4, 5, 6, 7, 8], the phase-space generation and the theoretical models for the QED processes $e^-e^+ \rightarrow \mu^+\mu^-(n\gamma)$ and $e^-e^+ \rightarrow \tau^+\tau^-(n\gamma)$ and decays of the τ lepton. The phase-space generators are extensions of the algorithm from [9] modified to include embedded importance sampling [10, 11] constructed in terms of the structure of the relevant physics models to optimize the simulation. The QED cross-section for $e^-e^+ \rightarrow \mu^+\mu^-(n\gamma)$ and $e^-e^+ \rightarrow \tau^+\tau^-(n\gamma)$ is determined within the Yennie-Frautschi-Suura Exponentiation Formalism [12],

$$d\sigma = \frac{\sum_{n=0}^{\infty} Y_i(Q_i^2) Y_f(Q_f^2) |\sum_{k=1}^{\infty} \bar{\mathcal{M}}_a^b|^2 dPS_a^{\delta M}}{4(|\vec{P}_{e^-}|E_{e^+} + E_{e^-}|\vec{P}_{e^+}|)} \quad (1)$$

where the matrix elements are computed directly from the Feynman Diagrams using an object-orientated formalism [3]. $Y_{i/f}(Q_i^2)$ represents the initial-state/final-state Yennie-Frautschi-Suura Exponentiation which has been implemented for: the Yennie-Frautschi-Suura calculation [12]; the KK2F approximation [13]; Sudakov Form-Factor [14]; and the Full LO calculation from [15] applying corrections from [3, 14, 16] for the Coulomb potential. Renormalization is incorporated into the running of electromagnetic coupling constant [17, 18] by means of Wards Identity [19]. Details for the renormalization and Exponentiation in eeMC can be found in [3]. The τ decays are simulated for both leptonic, $\tau^- \rightarrow l^- \bar{\nu}_l \nu_\tau^1$, and semi-leptonic decays, $\tau^- \rightarrow h_x \nu_\tau$, at Born level. The hadronic currents are implemented in the context of several theoretical frame-works: Chiral-Resonance-Lagrangian Models [20, 21, 22, 23]; ‘‘Chromoelectric Flux-Tube Breaking Model’’ within a ‘‘revitalized [3P_0] quark

*Corresponding Author

Email: inugent.physics@outlook.com

¹The Charge conjugate is implied throughout this paper.

model(s)” [24, 25, 26, 27, 28]; Vector-Dominance Models [29, 30]; and phenomenological models [31, 32, 33].

3 Initial State Polarization and the Spin Algorithm

The beam polarizations can be characterized in terms of the polarimetric vector ($\vec{\mathbf{P}}$) representing the average spin direction of the interacting initial state electron or positron in the center-of-mass (CM) reference frame. The magnitude $|\vec{\mathbf{P}}|$ represents the strength of polarization or probability of the electron or positron being in a polarized state. In terms of the quantum mechanical spin-projection operator, the expectation value for the polarization vector may be written as

$$\begin{aligned} \langle S_{\hat{\mathbf{n}}} \rangle &= \langle s_{1/2,m} | \hat{S}_{\hat{\mathbf{n}}} | s_{1/2,m} \rangle \\ &= \langle s_{1/2,m} | \frac{\hbar}{2} (n_x \hat{\sigma}_x + n_y \hat{\sigma}_y + n_z \hat{\sigma}_z) | s_{1/2,m} \rangle \end{aligned} \quad (2)$$

where $\hat{\mathbf{n}}$ is a unit vector defined by $\vec{\mathbf{P}} = |\vec{\mathbf{P}}| \times \hat{\mathbf{n}}$. The wave-function of the electron and positron corresponding to a spin aligned along the polarimetric vector can be constructed by means of a linear super-positioning of the longitudinal helicity states using the two orthogonal eigen-vectors of the spin-projection operators $\hat{S}_{\hat{\mathbf{n}}} = \frac{\hbar}{2} (n_x \hat{\sigma}_x + n_y \hat{\sigma}_y + n_z \hat{\sigma}_z)$ corresponding to the polarimetric vector. The generalized eigen-vector with $+1(a_{\hat{\mathbf{n}}})$ and $-1(b_{\hat{\mathbf{n}}})$ eigen-values may be written as

$$a_{\hat{\mathbf{n}}} = \begin{pmatrix} \cos(\frac{\theta}{2}) \\ \sin(\frac{\theta}{2}) e^{i\phi} \end{pmatrix}, \quad b_{\hat{\mathbf{n}}} = \begin{pmatrix} \sin(\frac{\theta}{2}) \\ -\cos(\frac{\theta}{2}) e^{i\phi} \end{pmatrix} \quad (3)$$

respectively. In the context of the modified Altarelli-Parisi Density Function, from which the spin algorithms in $ee \in MC$ are based, the linear super-position of states is incorporated in the spin sum through the projection operators [19, 34]. Adapting the initial state of the modified Altarelli-Parisi Density Function from [34, 35, 36] to include the Pauli-spin operator corresponding to the polarimetric vectors yields

$$\rho_{\lambda_i, \lambda_{i'}}^{(e^-)} \rho_{\lambda_j, \lambda_{j'}}^{(e^+)} \times \mathcal{M}_{a\lambda_i, \lambda_j, \lambda_k, \lambda_l, \dots, \lambda_n}^b \mathcal{M}_{a\lambda_{i'}, \lambda_{j'}, \lambda_{k'}, \lambda_{l'}, \dots, \lambda_n}^{b*} \times \prod_{\alpha=k}^n D_{\lambda_\alpha, \lambda'_\alpha} \quad (4)$$

where $\rho_{\lambda_i, \lambda_{i'}}^{(e^-)}$ ($\rho_{\lambda_j, \lambda_{j'}}^{(e^+)}$) are related to the $SU(2)$ representation of polarimetric vector [34] corresponding to the e^- (e^+) and are constructed from the weighted eigen-vectors for the $SU(2)$ Pauli-spin operators. The representation employed for the polarimetric vector of the initial state leptons is

$$\vec{\mathbf{P}} = F_p \hat{\mathbf{n}} = \begin{pmatrix} F_p \sqrt{1 - (P_l/F_p)^2} \cos(\phi_{\hat{\mathbf{n}}}) \\ F_p \sqrt{1 - (P_l/F_p)^2} \sin(\phi_{\hat{\mathbf{n}}}) \\ P_l \end{pmatrix} \quad (5)$$

and is defined in terms of two parameters, the $\phi_{\hat{\mathbf{n}}}$ of the lepton in the transverse ($x - y$) plane² and polarization

²Note, the definition for the angle $\phi_{\hat{\mathbf{n}}}$ for both the e^- and e^+ is in the CM frame coordinates where the P_l is defined along relative to the momentum of the e^- (e^+), the \hat{z} ($-\hat{z}$) axis.

fraction (F_p), in addition to the longitudinal polarization ($P_l = \cos(\theta) \times F_p$). The F_p allows for the inclusion of both unpolarized contributions when defining an arbitrary spin vector for the super-positioning of the spinor states and must necessarily be $P_l \leq F_p \leq 1$. P_l , $\phi_{\hat{\mathbf{n}}}$ and F_p can be defined on an event by event basis for both the initial e^- and e^+ leptons allowing for a distribution of spin states. This allows for the inclusion of changing polarization conditions, in particular tails caused by mis-alignment, spin relaxation distributions or radiative effects. From the latter form of the modified Altarelli-Parisi Density Function, the corresponding normalized spin probability is defined as

$$P_a^b = \rho_{\lambda_i, \lambda_{i'}}^{(e^-)} \rho_{\lambda_j, \lambda_{j'}}^{(e^+)} \times \frac{\mathcal{M}_{a\lambda_i, \lambda_j, \lambda_k, \lambda_l, \dots, \lambda_n}^b \mathcal{M}_{a\lambda_{i'}, \lambda_{j'}, \lambda_{k'}, \lambda_{l'}, \dots, \lambda_n}^{b*}}{|\mathcal{M}|^2} \times \prod_{\alpha=k}^n D_{\lambda_\alpha, \lambda'_\alpha} \quad (6)$$

where following the procedure from [3], the normalized real spin probability density function is determined by applying the completeness-relation and projection operators to the outgoing τ^-/τ^+ states and decay matrices [19, 34]. Alternatively, a change of basis can be applied to the initial state spinors by directly constructing the spinor states out of a super-positioning of the helicity states using a weighting of the orthogonal eigen-vectors for the spin-projection operator corresponding to the polarimetric vector. The algorithms in [3], were extended to include both the modified Altarelli-Parisi Density Function extended to include the $SU(2)$ representation of polarimetric vector for the e^-e^+ pair, as well as, the direct super-positioning of the helicity states³. The longitudinal factorized approach is modified to:

1. The given $e^+e^- \rightarrow l^+l^-(n\gamma)$ scattering process at order n , including the exponentiation procedure [3], is simulated using the spin-average summed matrix element,

$$|\mathcal{M}_a^b|^2 = \rho_{\lambda_i, \lambda_{i'}}^{(e^-)} \rho_{\lambda_j, \lambda_{j'}}^{(e^+)} \times \mathcal{M}_{a\lambda_i, \lambda_j, \lambda_k, \lambda_l, \dots, \lambda_n}^b \mathcal{M}_{a\lambda_{i'}, \lambda_{j'}, \lambda_{k'}, \lambda_{l'}, \dots, \lambda_n}^{b*} \quad (7)$$

where indices a and b represent the number of radiated hard photons and internal photon lines respectively. For the super-positioning case, the helicity state indices in the spin sum corresponds to the change of basis into the eigen-vector of the spin-operator $\hat{S}_{\hat{\mathbf{n}}}$ where $\lambda_i = \lambda_{i'}$ and $\lambda_j = \lambda_{j'}$.

2. The probability distribution P_{λ_k, λ_l} is determined by contracting only the initial state indices in the modified Altarelli-Parisi Density Function 4, where $\lambda_k = \lambda'_k$ and $\lambda_l = \lambda'_l$. An accept/reject algorithm is then applied using P_{λ_k, λ_l} to select the final state helicities with which the τ decays are simulated. The probability distribution P_{λ_k, λ_l} is computed in the longitudinal basis for the outgoing leptons for both cases and is independent of the initial state basis applied in the spin sum.

³The two approaches are included in the $ee \in MC$ as a means of verifying the numerical implementation. Both methods are theoretically equivalent.

3. Once the event is simulated, the transverse spin correlations are then included by means of a second accept/reject algorithm using the probability from the modified Altarelli-Parisi Density Function adapted to include the transverse initial-state spin effects, Eq. 6, which is bounded by $0 \leq P \leq 4$. At each step in the accept/reject algorithm, a random number is used for each τ lepton to rotate the τ decay products about the longitudinal axis of the respective τ , and the probability from the modified Altarelli-Parisi Density Function based on Eq. 6, is recomputed.

In the non-factorized approach:

1. The given $e^+e^- \rightarrow l^+l^-(n\gamma)$ scattering process at order n , including the exponentiation procedure [3], is simulated for the spin-average summed matrix element using the same procedure as the factorized approach.
2. The outgoing τ leptons are then decayed in an unpolarized state.
3. The spin structure is implemented in the simulate using an accept/reject algorithm based on the probability from the modified Altarelli-Parisi Density Function in Eq. 6. The final state decay products for each τ decay are rotated by a random ϕ and θ in the CM frame of respective τ decay before recomputing the probability from the modified Altarelli-Parisi Density Function adapted to include the transverse spin components of the initial state.

4 Impact on the Differential Cross-section and Correlation in τ Decays

At relativistic energies, the total cross-sections are found to be independent of the transverse polarization of the initial state polarization which is consistent with known ultra-relativistic spin sum calculations and trace theorems for Dirac spinors in which the cross-section depends only on the longitudinal polarization independent of the basis [19, 37]. This is in contrast to the non-relativistic energy, $|P| \ll E^4$, where mass effects are dominant, the cross-section depends on the spin and is independent of the momentum direction, which is consistent with the non-relativistic quantum mechanics expectation for spin 1/2 particles. Moreover, the longitudinal spin observables in τ decays are independent of the transverse spin component as would be expected from the wave-function description where the transverse spin is formed from a linear combinations of equal spin up and spin down helicity states. This is illustrated with the longitudinal spin observables $M_{\pi\pi}$ [38] in Figure 1 for $\cos(\theta_\pi) > 0$ and $\cos(\theta_\pi) < 0$. However, there are several observables related to the transverse polarization which are found to have a non-negligible impact on experimentally accessible distributions. In particular, the transverse polarization in the initial state leptons can

⁴This is achieved by artificially taking the limit where the mass of the initial-state electron and positron approaches $\rightarrow \sim \sqrt{s}/2$.

generate polarization dependant oscillations in the ϕ distributions missing transverse energy as seen in Figures 1 and 2. This is related to the spin correlations in the decay of the τ lepton in which the neutrinos are aligned along the polarization axis in the transverse plane (Figure 2). For comparison, oscillations in the transverse momentum distributions from the p-wave emission of scalar mesons are expected in $e^+e^- \rightarrow \Upsilon(4s) \rightarrow B^+B^-/B^0\bar{B}^0$ production when there is a transverse spin component in the initial state.

5 Conclusions

A modified spin algorithm, which includes spin correlations, has been implemented in `eeMC` to allow for the inclusion of an arbitrary initial spin configuration of the electron-positron pair suitable for the proposed BELLE-II polarization upgrade to SuperKEKB [1, 2]. The algorithm can be updated on an event-by-event basis to allow for a distribution of spin states including tails caused by misalignment or spin relaxation distributions and to allow for the inclusion of changing detector conditions. The spin algorithm was implemented using both an extension to the modified Altarelli-Parisi Density Function to include the transverse spin of the initial state electron and positron as well as implementing a change of basis for the initial state wave-function of the colliding electron and positron. Both approaches yielded consistent results. The predictions are found to be consistent with theoretical expectations for the total cross-section and longitudinal observables.

Acknowledgement

GCC Version 4.8.5 was used for compilation and the plots are generated using the external program GNUplot [39].

References

- [1] D. M. Asner et al. SnowMass 2021 White Paper on Upgrading SuperKEKB with a Polarized Electron Beam: Discovery Potential and Proposed Implementation. arXiv: 2205.12847 [physics.acc-ph].
- [2] J. M. Roney. Upgrading SuperKEKB with Polarized e^- Beams. *PoS, ICHEP2020:699*, 2021. doi: 10.22323/1.390.0699.
- [3] I. M. Nugent. `eeMC`: Simulation of $e^+e^- \rightarrow \mu^+\mu^-(\gamma)$ and $e^+e^- \rightarrow \tau^+\tau^-(\gamma)$ Events. arXiv: 2202.02318 [hep-ph].
- [4] M. Matsumoto and T. Nishimura. Mersenne Twister: a 623-Dimensionally Equidistributed Uniform Pseudo-Random Number Generator. *ACM Trans. Model. Comput. Simul.*, 8:3–30, 1998. doi: 10.1145/272991.272995.
- [5] T. Nishimura. Tables of 64-bit Mersenne twisters. *ACM Trans. Model. Comput. Simul.*, 10:348–357, 2000. doi: 10.1145/369534.369540.
- [6] S. Harase and T. Kimoto. Implementing 64-bit Maximally Equidistributed F2-Linear Generators with Mersenne Prime Period. *ACM Trans. on Mathematical Software*, 44:1–11, 2018. doi: 10.1145/3159444.
- [7] S. Vigna. An Experimental Exploration of Marsaglia’s xorshift Generators, Scrambled. 2016.
- [8] D. E. Knuth. *The Art of Computer Programming Vol 2 (2nd Ed.)*. Addison-Wesley, Reading, USA, 1981.
- [9] E. Byckling and K. Kajantie. n-Particle Phase Space in Terms of Invariant Momentum Transfer. *Nucl. Phys. B*, 9:568–576, 1969. doi: 10.1016/0550-3213(69)90271-5.

- [10] Dani Gamerman and Hedibert F. Lopes. *Markov Chain Monte Carlo: Stochastic Simulation for Bayesian Inference 2nd ed.* Chapman & Hall/CRC Taylor & Francis Group, 2006.
- [11] Andrew Gelman, John B. Carlin, Hal S. Stern, David B. Dunson, Aki Vehtari, and Donald B. Rubin. *Bayesian Data Analysis 3rd Ed.* CRC Press Taylor & Francis Group, 2014.
- [12] D. R. Yennie, S. C. Frautschi, and H. Suura. The Infrared Divergence Phenomena and High-Energy Processes. *Annals of Physics*, 13:379–452, 1961. doi: 10.1016/0003-4916(61)90151-8.
- [13] S. Jadach, B.F.L. Ward, and Z. Wąs. The Precision Monte Carlo Event Generator KK For Two-Fermion Final States In e^+e^- Collisions. *Comput. Phys. Commun.*, 130:260–325, 2000. doi: 10.1016/S0010-4655(00)00048-5.
- [14] Michael E. Peskin and Daniel V. Schroeder. *An Introduction to Quantum Field Theory.* Addison-Wesley, Reading, USA, 1995. ISBN 978-0-201-50397-5.
- [15] J. Schwinger. *Particle, Sources, and Fields Volumes I-III.* Perseus Books Publishing, L.L.C., Reading, Massachusetts, USA, 1998.
- [16] B. Smith and M.B. Voloshin. $e^+e^- \rightarrow \tau^+\tau^-$ at Threshold and Beyond. *Phys. Lett. B*, 324(1):117–120, 1994. doi: 10.1016/0370-2693(94)00095-6.
- [17] Friedrich Jegerlehner. *The Anomalous Magnetic Moment of the Muon.* Springer Tracts in Modern Physics 226, Heidelberg, Germany, 2007.
- [18] Christian Sturm. Leptonic Contributions to the Effective Electromagnetic Coupling at Four-Loop Order in QED. *Nuclear Physics B*, 874(3):698–719, Sep 2013. ISSN 0550-3213. doi: 10.1016/j.nuclphysb.2013.06.009.
- [19] Franz Mandl and Graham Shaw. *Quantum Field Theory: Revised Edition.* John Wiley & Sons, Great Britain, 1 1985.
- [20] Markus Finkemeier and Erwin Mirkes. Tau Decays into Kaons. *Z. Phys. C*, 69:243–252, 1996.
- [21] J. H. Kühn and A. Santamaria. Tau Decays to Pions. *Z. Phys. C*, 48:445–452, 1990. doi: 10.1007/BF01572024.
- [22] S. Jadach, Z. Wąs, R. Decker, and J. H. Kühn. The τ Decay Library TAUOLA: Version 2.4. *Comput. Phys. Commun.*, 76: 361–380, 1993. doi: 10.1016/0010-4655(93)90061-G.
- [23] R. Decker, E. Mirkes, R. Sauer, and Z. Wąs. Tau Decays into Three Pseudoscalar Mesons. *Z. Phys. C*, 58:445–452, 1993. doi: 10.1007/BF01557702.
- [24] Nathan Isgur, Colin Morningstar, and Cathy Reader. The a_1 in τ Decay. *Phys. Rev. D*, 39:1357, 1989. doi: 10.1103/PhysRevD.39.1357.
- [25] S. Godfrey and Nathan Isgur. Mesons in a Relativized Quark Model with Chromodynamics. *Phys. Rev. D*, 32:189–231, 1985. doi: 10.1103/PhysRevD.32.189.
- [26] Richard Kokoski and Nathan Isgur. Meson Decays by Flux Tube Breaking. *Phys. Rev. D*, 35:907, 1987. doi: 10.1103/PhysRevD.35.907.
- [27] N. Isgur and J.E. Paton. A Flux Tube Model for Hadrons. *Phys. Lett. B*, 124:247–251, 1983. doi: 10.1016/0370-2693(83)91445-4.
- [28] N. Isgur and J.E. Paton. A Flux Tube Model for Hadrons in QCD. *Phys Rev D.*, 31:2910, 1984. doi: 10.1103/PhysRevD.31.2910.
- [29] A.E. Bondar, S.I. Eidelman, A.I. Milstein, T. Pierzchała, N.I. Root, Z. Wąs, and M. Worek. Novosibirsk Hadronic Currents for $\tau \rightarrow 4\pi\nu$ Channels of τ Decay Library TAUOLA. *Computer Physics Communications*, 146(2):139 – 153, 2002. ISSN 0010-4655. doi: 10.1016/S0010-4655(02)00262-X.
- [30] A. E. Bondar, S. I. Eidelman, A. I. Milstein, and N. I. Root. On the Role of the $a_1(1260)$ Meson in $\tau \rightarrow 4\pi\nu_\tau$ Decays. *Phys. Lett. B*, 466(2-4):403–407, 1999. doi: 10.1016/s0370-2693(99)01081-3.
- [31] D. M. Asner et al. Hadronic Structure in the Decay $\tau^- \rightarrow \nu_\tau \pi^- \pi^0 \pi^0$ and the Sign of the Tau Neutrino Helicity. *Phys. Rev. D*, 61:012002, Dec 1999. doi: 10.1103/PhysRevD.61.012002.
- [32] K.W. Edwards et al. Resonant Structure of $\tau \rightarrow 3\pi^0 \nu_\tau$ and $\tau \rightarrow \omega \pi \nu_\tau$ Decays. *Phys. Rev. D*, 61:072003, 2000. doi: 10.1103/PhysRevD.61.072003.
- [33] M. Feindt. Measuring Hadronic Currents and Weak Coupling Constants in $\tau \rightarrow$ Neutrino 3π . *Z. Phys. C*, 48:681–688, 1990. doi: 10.1007/BF01614704.
- [34] S. Jadach and Z. Wąs. QED $\mathcal{O}(\alpha^3)$ Radiative Corrections to the Reactions $e^+e^- \rightarrow \tau^+\tau^-$ Including Spin and Mass Effects. *Acta Phys. Polon. B*, 15:1151, 1984. [Erratum: *Acta Phys. Polon. B* 16 (1985) 483].
- [35] J. C. Collins. Spin Correlations in Monte Carlo Event Generators. *Nucl. Phys. B*, 304:794–804, 1987. doi: 10.1016/0550-3213(88)90654-2.
- [36] I. G. Knowles. A Linear Algorithm for Calculating Spin Correlations in Hadronic Collisions. *Comput. Phys. Commun*, 58: 271–284, 1990. doi: 10.1016/0010-4655(90)90063-7.
- [37] F. Halzen and Alan D. Martin. *Quarks And Leptons: An Introductory Course In Modern Particle Physics.* John Wiley & Sons, USA, 1 1984. ISBN 978-0-471-88741-6.
- [38] T. T. Pierzchała, E. Richter-Wąs, Z. Wąs, and M. Worek.
- [39] Thomas Williams, Colin Kelley, et al. Gnuplot 4.2: An Interactive Plotting Program. <http://gnuplot.sourceforge.net/>, 2007.

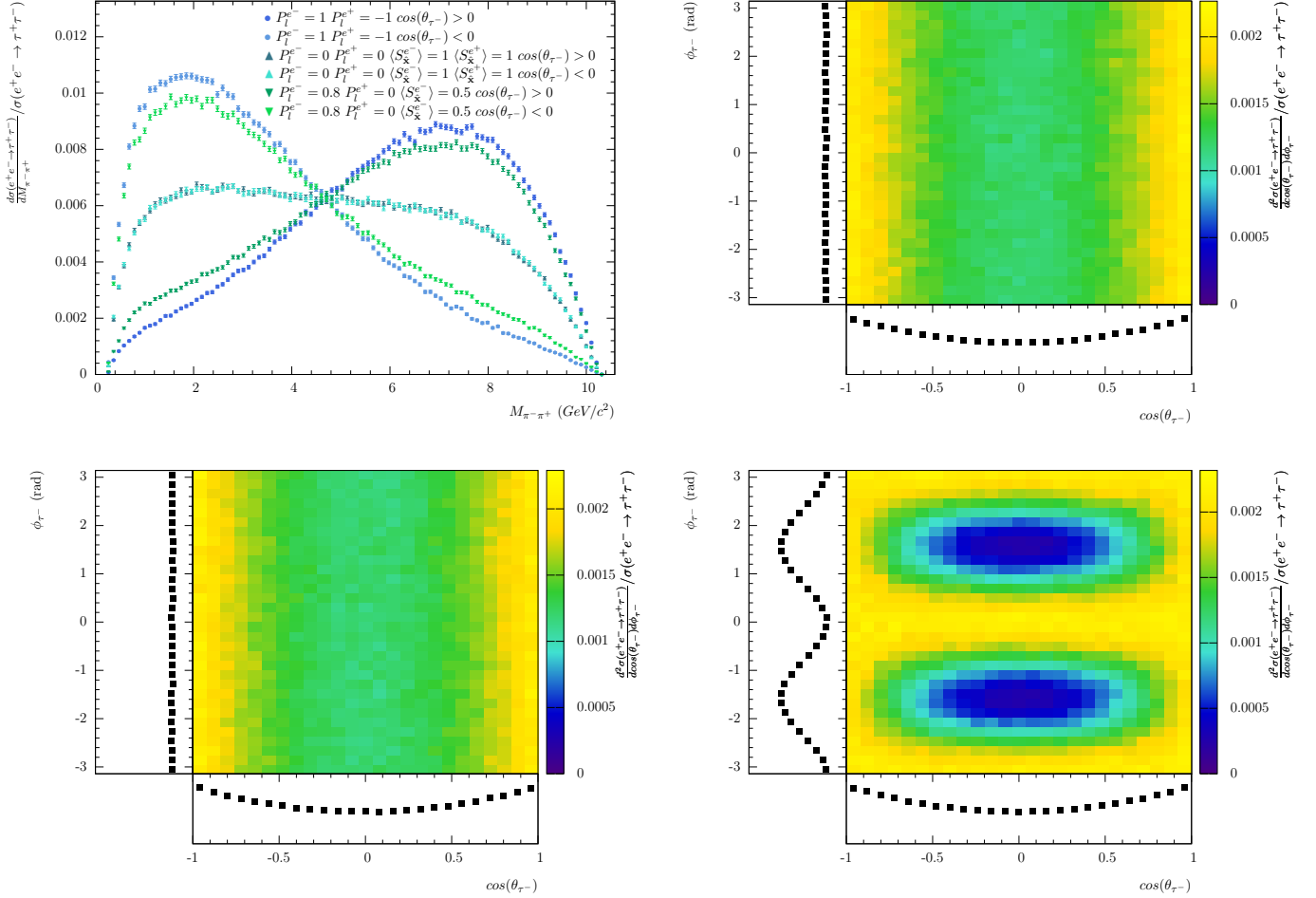


Figure 1: The longitudinal observable $M_{\pi^+\pi^-} \cos(\theta_{\tau^-}) > 0$ and $\cos(\theta_{\tau^-}) < 0$ distributions (upper-left) for longitudinally polarized beams, for a transversely polarized beam, and for a realistic polarization scenario at the proposed polarization upgrade at Belle-II [1]. There is a strong dependence between the $\cos(\theta_{\tau^-}) > 0$ and $\cos(\theta_{\tau^-}) < 0$ distributions for the longitudinally polarized sample, while the transversely polarized sample is independent of $\cos(\theta_{\tau^-}) > 0$ and $\cos(\theta_{\tau^-}) < 0$. The cross-section as a function $\cos(\theta_{\tau^-})$ and ϕ_{τ^-} for a 100% longitudinally polarized e^+ and e^- sample (lower-left) and for a 100% transversely polarized (along the x-axis) e^+ and e^- sample (lower-right) and for a realistic polarization scenario at the proposed polarization upgrade at Belle-II [1] (upper-right). To simplify the interpretation of these diagrams, they have been simulated at Born level.

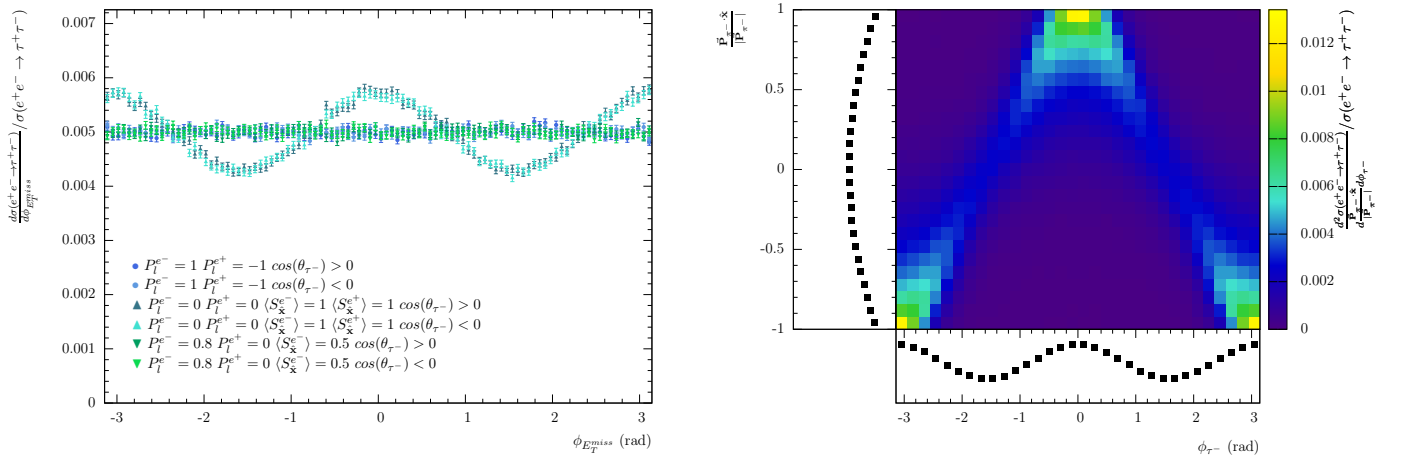


Figure 2: An overlay of the missing transverse momentum (left) in a 100% longitudinal polarized sample and for 100% transversely polarized (along the x-axis) e^+ and e^- sample along with the $\cos(\theta_{\pi^-})$ ϕ_{π^-} dependence of the cross-section weighted by $\frac{\vec{P}_{\pi^-} \cdot \hat{x}}{|\vec{P}_{\pi^-}|}$. To simplify the interpretation of these diagrams, they have been simulated at Born level.